



## Radon Decay Product Aerosols in Ambient Air

Constantin Papastefanou\*

Atomic and Nuclear Physics Laboratory, Aristotle University of Thessaloniki, Thessaloniki 54124, Greece

### ABSTRACT

The aerodynamic size distributions of radon decay product aerosols, i.e.  $^{214}\text{Pb}$ ,  $^{212}\text{Pb}$ , and  $^{210}\text{Pb}$  were measured using low-pressure (LPI) as well as conventional low-volume 1-ACFM and high-volume (HVI) cascade impactors. The activity size distribution of  $^{214}\text{Pb}$  and  $^{212}\text{Pb}$  was largely associated with submicron aerosols in the accumulation mode (0.08 to 2.0  $\mu\text{m}$ ). The activity median aerodynamic diameter “AMAD” varied from 0.10 to 0.37  $\mu\text{m}$  (average 0.16  $\mu\text{m}$ ) for  $^{214}\text{Pb}$ -aerosols and from 0.07 to 0.25  $\mu\text{m}$  (average 0.12  $\mu\text{m}$ ) for  $^{212}\text{Pb}$ -aerosols. The geometric standard deviation,  $\sigma_g$  averaged 2.86 and 2.97, respectively. The AMAD of  $^{210}\text{Pb}$ -aerosols varied from 0.28 to 0.49  $\mu\text{m}$  (average 0.37  $\mu\text{m}$ ) and the geometric standard deviation,  $\sigma_g$  varied from 1.6 to 2.1 (average 1.9). The activity size distribution of  $^{214}\text{Pb}$ -aerosols showed a small shift to larger particle sizes relative to  $^{212}\text{Pb}$ -aerosols. The larger median size of  $^{214}\text{Pb}$ -aerosols was attributed to  $\alpha$ -recoil depletion of smaller aerosol particles following the decay of the aerosol-associated  $^{218}\text{Po}$ . Subsequent  $^{214}\text{Pb}$  condensation on all aerosol particles effectively enriches larger-sized aerosols. Pb-212 does not undergo this recoil-driven redistribution. Even considering recoil following  $^{214}\text{Po}$   $\alpha$ -decay, the average  $^{210}\text{Pb}$ -labeled aerosol grows by a factor of two during its atmospheric lifetime. Early morning and afternoon measurements indicated that similar size associations of  $^{214}\text{Pb}$  occur, despite humidity differences and the potential for fresh particle production in the afternoon. In estimating lifetimes of radon decay product aerosols in ambient air, a mean residence time of about 8 days could be applied to aerosol particles in the lower atmosphere below precipitation cloud levels.

**Keywords:** Radon; Decay products;  $^{214}\text{Pb}$ ;  $^{212}\text{Pb}$ ;  $^{210}\text{Pb}$ ; Radioactive aerosols; Cascade impactors; 1-ACFM; AMAD; Residence time.

### INTRODUCTION

The decay of radon,  $^{222}\text{Rn}$  and thoron,  $^{220}\text{Rn}$  in the atmosphere produces low vapor pressure decay products that coagulate with other nuclei or condense on existing aerosol particles. These decay products include  $^{218}\text{Po}$  (3.0 min),  $^{214}\text{Pb}$  (26.8 min) and  $^{212}\text{Pb}$  (10.64 h). A long-lived decay product in the  $^{222}\text{Rn}$  decay chain,  $^{210}\text{Pb}$  (22.3 y) is produced about an hour after attachment of  $^{218}\text{Po}$  onto aerosol particles. Very little data exist on the ambient aerosol associations of the decay products of both radon isotopes with respect to their aerodynamic size distributions relative to the formation and growth mechanisms of aerosols.

Fig. 1 presents the decay scheme for radon,  $^{222}\text{Rn}$  and thoron,  $^{220}\text{Rn}$ , illustrating the short-lived as well as the long-lived decay products, their mode of radioactive decay and their half-lives.

Diffusion batteries have been used to investigate aerosol size associations of gross  $\alpha$ -activity from the short-lived radon decay products (Soilleux, 1970; George and Breslin, 1980; George *et al.*, 1984) in outdoor air situations, and high-volume cascade impactors for gross  $\beta$ - and  $\gamma$ -activity from the long-lived radon and thoron decay products (Röbüg *et al.*, 1980). The residence time of atmospheric aerosol particles in the lower atmosphere assuming that the air in the troposphere is considered as a well-mixed reservoir (closed system) is a function of various removal processes, the most important being:

- dry deposition by impaction, diffusion and sedimentation, and
- wet deposition by rain drops (precipitation scavenging) as a

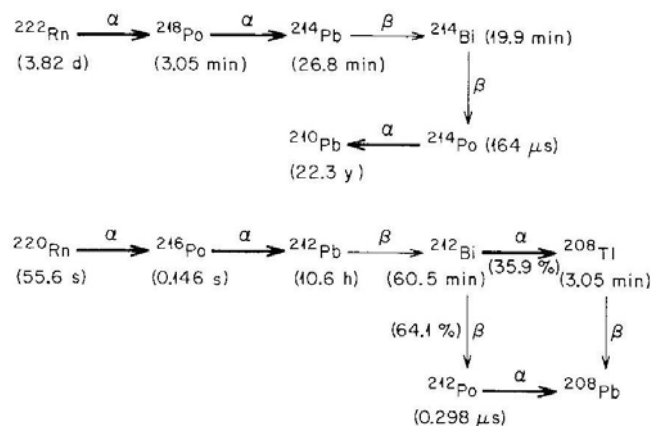


**Fig. 1.** Decay schemes of  $^{222}\text{Rn}$  and  $^{220}\text{Rn}$  illustrating short-lived and long-lived decay products.

result of processes occurring both within and below the rain cloud.

The residence time of atmospheric aerosol particles can be estimated by means of radioactive nuclides as tracers, which become attached to aerosol particles and are removed with them as they are scavenged by precipitation or undergo dry fallout. Several methods have been used for estimating the mean residence time of atmospheric aerosol particles. These include measurements of the activities and ratios of radioactive decay products of radon,  $^{222}\text{Rn}$  which emanate from continental surfaces into the atmosphere, such as  $^{210}\text{Pb}$  (22.3 y),  $^{210}\text{Bi}$  (5.01 d) and  $^{210}\text{Po}$  (138.38 d) (Francis *et al.*, 1970; Poet *et al.*, 1972; Lambert *et al.*, 1980; 1983; Marley *et al.*, 2000; Baskaran and Shaw, 2001). However, there is disagreement between the

\* Corresponding author. Tel.: +30-2310-998005;  
 Fax: +30-2310-998058  
 E-mail address: papastefanou@physics.auth.gr

derived values of the residence times due to various processes, including the fact that they refer to different portions of the atmosphere.

This paper summarizes results of an investigation designed to characterize the aerodynamic size distributions and the residence time of atmospheric aerosols in the context of  $^{222}\text{Rn}$ - and  $^{220}\text{Rn}$ -decay products for better understanding of how radioactive aerosols behave in the atmosphere, and of the aerosol growth mechanism.

## EXPERIMENTAL METHODS

Measurements on aerodynamic sizes of atmospheric aerosols associated with radioactive nuclides, such as radon decay products  $^{214}\text{Pb}$ ,  $^{212}\text{Pb}$  and  $^{210}\text{Pb}$  were carried with Anderson type 1-ACFM ambient cascade impactors with or without the Andersen model 2000 low-pressure modification, as well as with Sierra model 236, six-stage high-volume cascade impactors, HVI.

The 1-ACFM design operated at 28 L/min (1 ft<sup>3</sup>/min). The eight stages had effective cutoff diameters, ECDs of 0.4, 0.7, 1.1, 2.1, 3.3, 4.7, 7.0 and 11.0  $\mu\text{m}$ . The low-pressure modification, which alters the impactor's operation by increasing the resolution in the submicron region, involves a regulated flow rate of 3 L/min, five low-pressure (114 mm Hg) stages for the submicron region and eight atmospheric pressure stages for separating aerosol particles above 1.4  $\mu\text{m}$ . The ECDs of the low-pressure stages were 0.08, 0.11, 0.23, 0.52 and 0.90  $\mu\text{m}$ , whereas for the upper stages they were 1.4, 2.0, 3.3, 6.6, 10.5, 15.7, 21.7 and 35.0  $\mu\text{m}$ . A schematic diagram of a low-pressure cascade impactor, LPI complete system is shown in Fig. 2. The stainless steel plates supplied by the manufacturer were used for aerosol particle collection. Either polycarbonate or glass-fiber backup filters were used to collect all particles below the 0.08- $\mu\text{m}$  collection plate. The ECDs of the high-volume impactor stages were 0.41, 0.73, 1.4, 2.1, 4.2 and 10.2  $\mu\text{m}$ . The flow rate of this 20 cfm high-volume cascade impactor was about 34 m<sup>3</sup>/h.

The length of each collection period varied from about 3 h for  $^{214}\text{Pb}$  to 30 or 40 h for  $^{212}\text{Pb}$  with low-pressure impactor measurements and from 1 to 24 h for  $^{210}\text{Pb}$  and  $^{210}\text{Bi}$  for high-volume impactor measurements. The samples were collected 13 m above the ground on the roof of the Environmental Sciences

Division building at the Oak Ridge National Laboratory, ORNL, in Oak Ridge, Tennessee (35°58'N, 84°30'W).

The deposits on the stainless-steel collection plates of the low-pressure cascade impactor were leached with a solution of 1 M  $\text{HNO}_3$  and the leachate rapidly evaporated on 5.08-cm stainless steel plates using a hot plate. The concentrations of  $^{214}\text{Pb}$  and  $^{212}\text{Pb}$  in the impactor plate leachates were measured using seven ZnS (Ag) alpha scintillation counters with backgrounds averaged 0.025 cpm. The  $1\sigma$  counting uncertainty was 5% or less for the stages corresponding to aerosols below 0.52  $\mu\text{m}$  and < 15% for the stages collecting to aerosols above 0.52  $\mu\text{m}$ . The calculated activities of  $^{214}\text{Pb}$  and  $^{212}\text{Pb}$  were used to determine the activity size distribution of each radionuclide and then the activity median aerodynamic diameter "AMAD" of the  $^{214}\text{Pb}$ - and  $^{212}\text{Pb}$ -aerosols. The high-volume impactor plates were leached with 0.1 M HCl. Lead-210 was determined 30 days after collection stopped by separating and measuring  $^{210}\text{Bi}$  (Poet *et al.*, 1972). When  $^{210}\text{Pb}$  was measured, the upper two high-volume impactor stages were coated with a thin layer of petroleum jelly to minimize soil particle bounce. While nucleopore polycarbonate membranes (0.4  $\mu\text{m}$ ) were preferred as backup filters for low-pressure cascade impactors, glass-fiber filters had to be used in the high-volume impactor measurements.

The activity of  $^{210}\text{Pb}$ - and  $^{210}\text{Bi}$ -associated aerosol particles was measured by a low-background phoswich scintillation detector system having a background of 2 cpm and efficiency higher than 40% for counting  $\beta$ -radiation. This system consisted of a thin  $\text{CaF}_2$  (Eu) primary crystal with a decay time of 0.23  $\mu\text{s}$ . The samples were counted for long enough to obtain a statistical accuracy better than 5%. It must be noted that  $^{210}\text{Pb}$  and  $^{210}\text{Bi}$  were chemically separated and measured for their activities. Detailed description of the analytical method and technique was established and presented elsewhere (Jaworowski, 1963). The activity of  $^{210}\text{Pb}$  was also measured by a surface barrier Ge detector through its gamma-ray peak of 46.5 keV. The activity size distribution and the AMAD of the  $^{210}\text{Pb}$ -aerosol particles were determined upon the measurement of the activities of the aerosol-associated radioactive nuclides. Fig. 3 shows a typical gamma-ray spectrum of a glass fiber air filter obtained by a Ge detector, in which the 46.5 keV  $\gamma$ -ray peak of  $^{210}\text{Pb}$  is clearly shown.

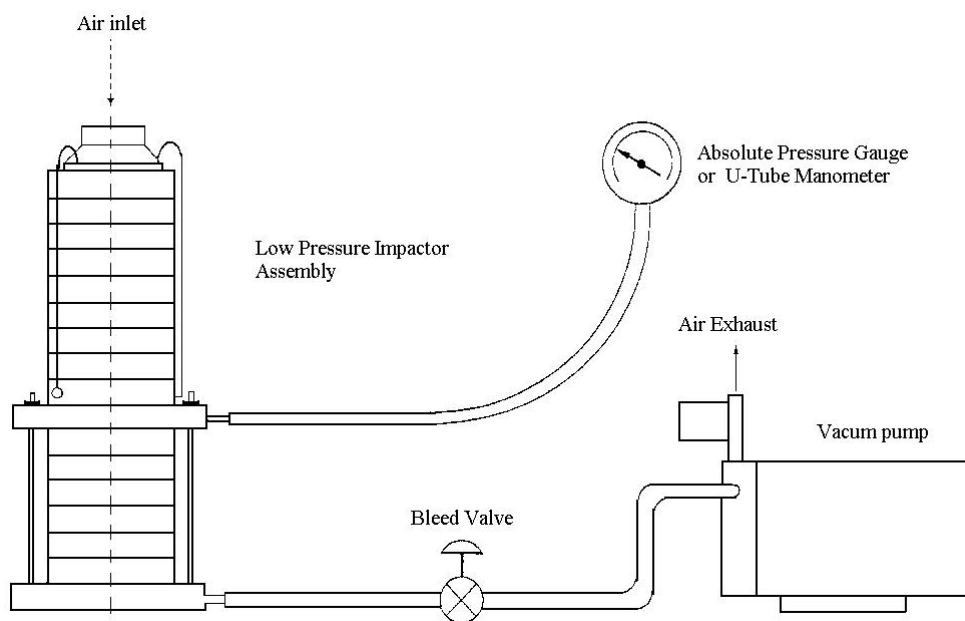


Fig. 2. A schematic diagram of a low-pressure cascade impactor complete system.

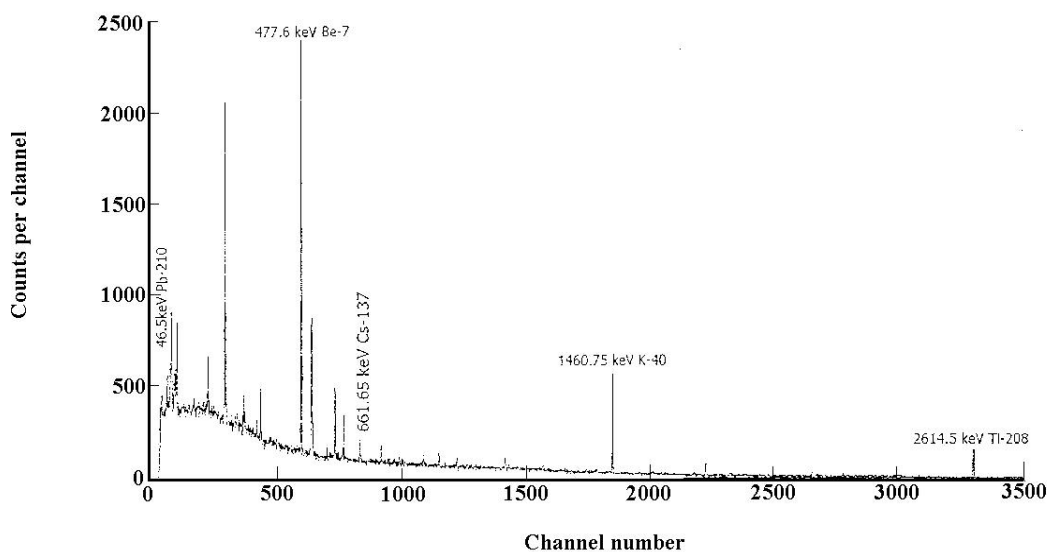


Fig. 3. Plot of a  $\gamma$ -ray spectrum of an atmospheric aerosol sample (air filter) obtained by a Ge detector.

## RESULTS AND DISCUSSION

### Activity Size Distribution of Radon Decay Product Aerosols

Fig. 4 shows representative plots from 46 low-pressure impactor measurements made over a ten-month period, illustrating the aerodynamic size distributions of  $^{214}\text{Pb}$ - and  $^{212}\text{Pb}$ -aerosols.  $R$  is the radioactivity and  $D_p$  is the particle diameter, in  $\mu\text{m}$ .

About 46% of the measurements showed a radioactivity peak in the 0.11- to 0.23- $\mu\text{m}$  region (subplot a), while 39% showed a peak in the 0.23- to 0.52- $\mu\text{m}$  region (subplot b). The remaining 15% of the measurements resulted in activity size distributions similar to those in subplot c (8.7%) or subplot d (6.5%), where  $^{214}\text{Pb}$ - and  $^{212}\text{Pb}$ - activities were highest in different size ranges in the same spectrum. On the average, about 76% of the  $^{214}\text{Pb}$ -activity and 67% of the  $^{212}\text{Pb}$ -activity was found to be associated with aerosol particles in the 0.08- to 1.4- $\mu\text{m}$  size range. The activity- associated with aerosol particles smaller than 0.08- $\mu\text{m}$  can also be substantial, as indicated in Fig. 4. Fig. 4 illustrates that  $^{214}\text{Pb}$  is generally enriched in the accumulation mode aerosol, particularly between 0.11 and 0.52  $\mu\text{m}$ , where most of the surface area and mass occurs, while the Aitken nuclei fraction (below 0.08  $\mu\text{m}$ ) contained a higher percentage of  $^{212}\text{Pb}$ -activity compared with  $^{214}\text{Pb}$ -activity in 69.6% of the measurements.

The radon decay products become associated with atmospheric aerosol particles by condensation or coagulation processes that are surface-area related. The activity size distribution of  $^{214}\text{Pb}$ -aerosols showed a small shift to larger particle sizes relative to  $^{212}\text{Pb}$ -aerosols. The shift of  $^{214}\text{Pb}$  to a slightly higher size distribution compared to  $^{212}\text{Pb}$  was also found using 1-ACFM and high-volume cascade impactors (Fig. 5). The higher flow rates of these impactors, as well as the ability to measure high-volume activity by gamma-ray spectrometry, made us confident that this shift was real and not a data analysis artifact. The larger median size of  $^{214}\text{Pb}$ -aerosols was attributed to  $\alpha$ -recoil depletion of smaller aerosol particles following the decay of the aerosol-associated  $^{218}\text{Po}$ . Subsequent  $^{214}\text{Pb}$  condensation on all particles effectively enriches larger-sized aerosols. Pb-212 does not undergo this recoil-driven redistribution. Even considering recoil following  $^{214}\text{Po}$   $\alpha$ -decay, the average  $^{210}\text{Pb}$ -labelled aerosol grows by a factor of two during its atmospheric lifetime. Early morning and afternoon measurements indicated that similar size associations of  $^{214}\text{Pb}$  occur, despite humidity differences and the potential for fresh particle production in the afternoon.

The longer half-life of  $^{212}\text{Pb}$  (10.64 h) compared to  $^{214}\text{Pb}$  (26.8 min) might favor the presence of larger aerosol associations of  $^{212}\text{Pb}$  if coagulation rates are fast relative to radioactive decay rates, although cascade impactor measurements may not be sensitive enough to record this effect. Instead, the measurements indicated that the shorter-lived chain ( $^{218}\text{Po}$ ,  $^{214}\text{Pb}$ , etc) was more often associated with larger aerosol particle sizes than the longer-lived chain ( $^{216}\text{Po}$ ,  $^{212}\text{Pb}$ , etc). The high-volume impactor measurements reported by R6big *et al.* (1980) also indicated a large particle shift of  $^{214}\text{Pb}$  relative to  $^{212}\text{Pb}$  (Fig. 6). They stated that this was due to shifts of the activity size distributions from night to day-time to smaller particle sizes by photochemical reactions and to shifts to larger particle sizes when the relative humidity increases during rainfall, and therefore depends on sampling time. They also observed that the activity size distributions of the long-lived radionuclides  $^{210}\text{Pb}$  and  $^7\text{Be}$  are shifted to larger particle sizes compared with the activity size distributions of the shorter-lived  $^{214}\text{Pb}$  and  $^{212}\text{Pb}$ . That shift was due to larger residence times for  $^{210}\text{Pb}$  and  $^7\text{Be}$  in the atmosphere and for  $^7\text{Be}$  due to a different size distribution of stratospheric and tropospheric aerosols.

The  $^{214}\text{Pb}$  shift might be explained by the fact that a significant fraction of the 3.05-min  $^{218}\text{Po}$  atoms, precursor of  $^{214}\text{Pb}$  atoms should attach to an existing aerosol particle or coagulate with other nuclei during their lifetime, as mean attachment half-lives are of the order of a minute less (Porstend6rfer and Mercer, 1980). When this attached  $^{218}\text{Po}$   $\alpha$ -decays, the recoiling  $^{214}\text{Pb}$  atom, decay product of  $^{218}\text{Po}$ , can escape the aerosol particles. Complete recoil loss would occur if the particle diameter,  $D_p$  of the aerosol were smaller than the range of the recoiling nucleus. In water, this recoil range is 0.13  $\mu\text{m}$  (Mercer, 1976) and should be somewhat less in the atmospheric aerosols that have a density closer to 1.5  $\text{g cm}^{-3}$  (Friedlander, 2000). By contrast, very little of the 0.146  $\mu\text{s}$   $^{216}\text{Po}$  would attach before decaying to  $^{212}\text{Pb}$ , because of its short life relative to attachment times. A considerable fraction of the  $^{214}\text{Pb}$  should undergo recoil detachment, particularly from aerosol particles with diameters smaller than 0.1  $\mu\text{m}$  (diameter approximating the recoil range). The probability of loss would decrease with increasing particle radius (Mercer, 1976). If the recondensing  $^{214}\text{Pb}$  behaves like the original  $^{214}\text{Po}$ , the net effect would be a shift of  $^{214}\text{Pb}$  to a larger particle size distribution.

Since the subsequent  $\beta$ -decays of  $^{212}\text{Pb}$  and  $^{214}\text{Pb}$  +  $^{214}\text{Bi}$  do not result in significant recoil (Mercer, 1976), the  $\alpha$ -measurement of

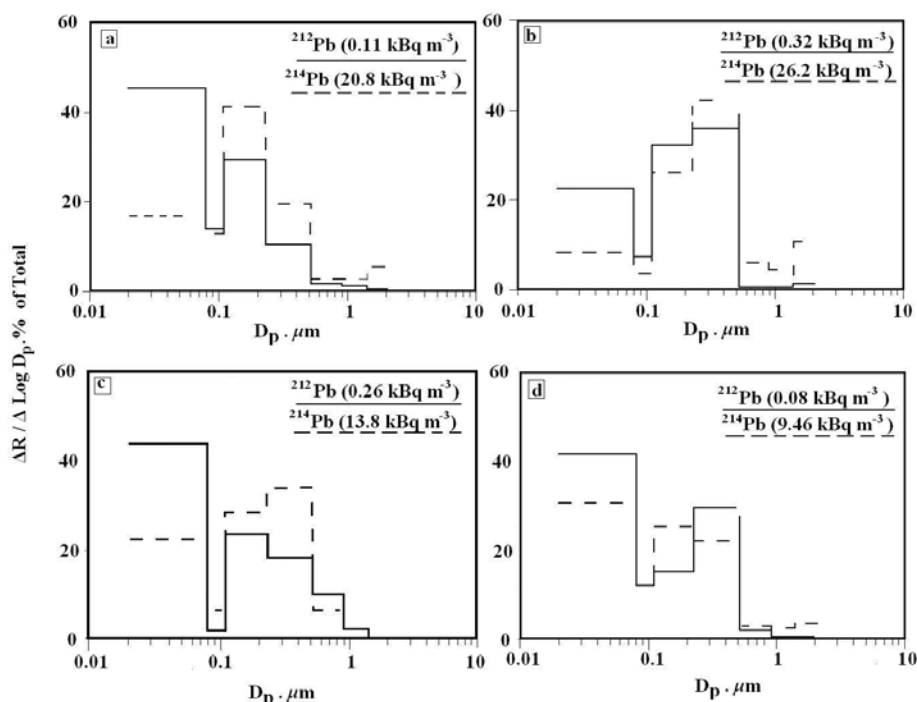


**Fig. 4.** Aerodynamic size distributions of  $^{214}\text{Pb}$ - and  $^{212}\text{Pb}$ -aerosols obtained with low-pressure cascade impactors. R is the radioactivity, and  $D_p$  is the particle diameter. (a) Results occurred 46% of the time, (b) 39% of the time, (c) 8.7% of the time, and (d) 6.5% of the time. Lower  $D_p$  limits are arbitrary.

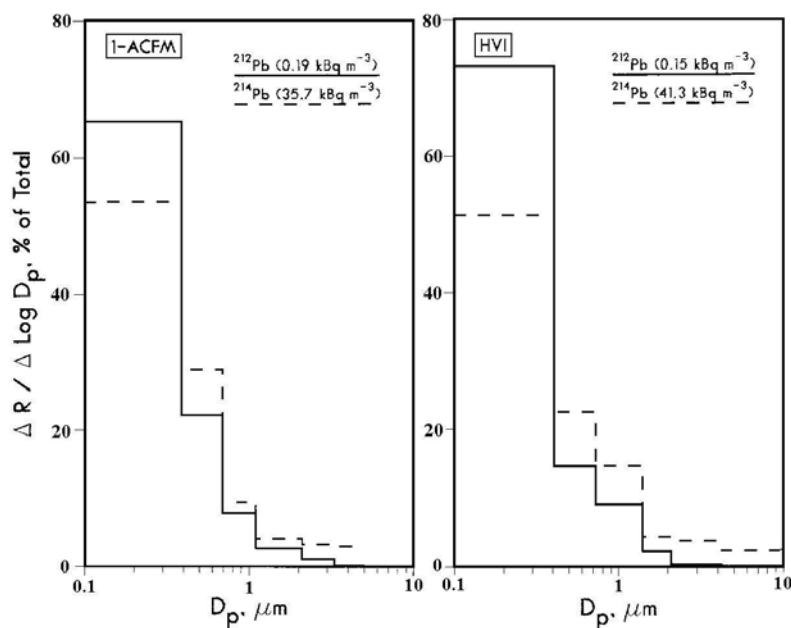


**Fig. 5.** Aerodynamic size distributions of  $^{214}\text{Pb}$ - and  $^{212}\text{Pb}$ -aerosols obtained with 1-ACFM and high-volume cascade impactors, illustrating the large particle shift of  $^{214}\text{Pb}$ . R is the radioactivity, and  $D_p$  is the particle diameter. Lower  $D_p$  limits are arbitrary.

$^{214}\text{Po}$  and the  $^{212}\text{Pb}$ -decay products is in reality tracing the aerosol size distribution of a  $^{220}\text{Rn}$ -decay product atom ( $^{212}\text{Pb}$ ) which has condensed only once and a  $^{222}\text{Rn}$ -decay product atom ( $^{214}\text{Pb}$ ) that has probably condensed more than once. This stability of the Pb-isotopes is the basis for the generic reference to  $^{212}\text{Pb}$  and  $^{214}\text{Pb}$  size distributions.

The AMADs of  $^{214}\text{Pb}$ -aerosols determined with the low-pressure impactor data varied from 0.10 to 0.37  $\mu\text{m}$  (average 0.16

$\mu\text{m}$ ) and for  $^{212}\text{Pb}$ -aerosols from 0.07 to 0.25  $\mu\text{m}$  (average 0.12  $\mu\text{m}$ ) (Table 1). For the  $^{210}\text{Pb}$ -aerosols the AMADs varied from 0.28 to 0.49  $\mu\text{m}$  (average 0.37  $\mu\text{m}$ ). Lead-210 is produced by  $\alpha$ -decay of  $^{214}\text{Po}$ , the event used to quantify  $^{214}\text{Pb}$  distributions on the low-pressure cascade impactors. While the relationship between the aerodynamic sizes of  $^{214}\text{Pb}$  and  $^{210}\text{Pb}$  is complicated because of the large differences in their atmospheric lifetimes,  $^{210}\text{Pb}$  has always found to be associated with aerosols larger than

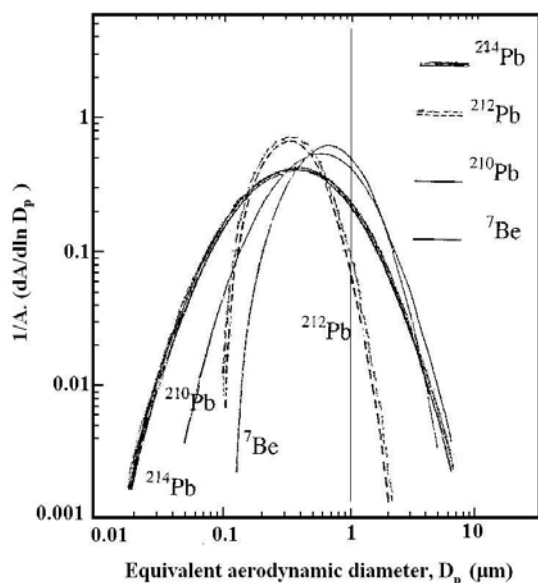


**Fig. 6.** The activity size distributions of the atmospheric aerosols in ambient air (Robig *et al.*, 1980).

$^{214}\text{Pb}$ , as indicated by the differences in AMADs reported in Table 1. Table 1 shows data for the AMADs of the radon decay product aerosols. The results were obtained assuming lognormal distributions. The reported from the literature data for radon decay product aerosols are also presented in Table 1 and analyzed as follows:

Grundel and Porstendörfer (2004) more recently carried out measurements in outdoor air at a northern latitude ( $51^{\circ}32'\text{N}$ ,  $9^{\circ}55'\text{E}$ ) in Göttingen, Germany using an on-line alpha cascade impactor (OLACI) for a period of about one month and showed that the activity size distributions of the short-lived radon ( $^{222}\text{Rn}$ ) and thoron ( $^{220}\text{Rn}$ ) decay products are about 12-19 % in the nucleation mode (Aitken nuclei, 0.05-60 nm), 81-88% in the accumulation size range (60-1000 nm), and with no coarse mode (particle diameter > 1000 nm). The AMAD of the accumulation mode varied between 332 nm for  $^{218}\text{Po}$  and 347 nm for  $^{214}\text{Po}$  for the short-lived radon decay products and between 382 nm for  $^{212}\text{Po}$  and 421 nm for  $^{212}\text{Pb}$  for the thoron decay products. In comparison to the short-lived radon decay products, the AMADs of the thoron decay products were shifted significantly to larger values. For the long-lived radon ( $^{222}\text{Rn}$ ) decay products  $^{210}\text{Pb}$  and  $^{210}\text{Po}$  they showed that these radionuclides are almost 93-96% adsorbed on aerosol particles in the accumulation size range and only 4-7% of their activities are attached on nuclei with diameters smaller than 60 nm. AMAD-values of 558 nm for  $^{210}\text{Pb}$  and 545 nm for  $^{210}\text{Po}$  were measured, i.e. significantly larger than those of the short-lived radon and thoron decay products.

In El-Minia, Egypt ( $28^{\circ}04'\text{N}$ ,  $30^{\circ}45'\text{E}$ ), El Hussein and

Ahmed (1995) by using a low-pressure Berner-type cascade impactor showed that the activity size distributions of the  $^{214}\text{Pb}$ - and  $^{214}\text{Bi}$ -attached aerosols were nearly identical and that most of the activities were associated with aerosol particles of the accumulation mode. The mean AMAD of  $^{214}\text{Pb}$ -aerosols (range 261-458 nm) and  $^{214}\text{Bi}$ -aerosols (range 190-620 nm) had the same value of 380 nm, but the relative geometric standard deviation,  $\sigma_g$ , of the log-normal distribution of  $^{214}\text{Pb}$ -aerosols ( $\sigma_g$ : 1.67-2.25, average 2.05) shows a broader activity size distribution than for  $^{214}\text{Bi}$ -aerosols ( $\sigma_g$ : 1.67-2.25, average 2.05). Later, El Hussein *et al.* (1998) from measurements in El-Minia, Egypt, found that the AMAD, varied from 175 to 485 nm (average 330 nm) and the geometric standard deviation,  $\sigma_g$ , varied from 1.62 to 3.21 (average 2.45) for  $^{214}\text{Pb}$ -aerosols and from 170 to 477 nm (average 316 nm) and  $\sigma_g$  from 1.79 to 3.12 (average 2.35) for  $^{214}\text{Bi}$ -aerosols. Apart from this, Mohammed (1999) by using a low-pressure Berner-type cascade impactor in El-Minia, Egypt reported that the AMAD for the very short-lived radon decay product  $^{218}\text{Po}$ -aerosols varied from 280 to 386 nm (average 340 nm) and the geometric standard deviation,  $\sigma_g$ , varied from 2.5 to 2.9 (average 2.7), while for its decay product  $^{214}\text{Pb}$ -aerosols the AMAD varied from 296 to 360 nm (average 320 nm) and the  $\sigma_g$  varied from 2.1 to 2.88 (average 2.7), which means that they are quite similar. For the relatively longer-lived thoron decay product  $^{212}\text{Pb}$ -aerosols, the AMAD of the accumulation mode varied from 249 to 390 nm (average 360 nm) and the  $\sigma_g$  varied from 2.1 to 3.2 (average 2.7) (Mohammed *et al.*, 2000).

Winkler *et al.* (1998) by using a nine-stage low-pressure Berner-type cascade impactor in Neuherberg, Germany ( $48^{\circ}13'\text{N}$ ,  $11^{\circ}36'\text{E}$ ) reported that the activity size distribution of  $^{210}\text{Pb}$  in ambient aerosols was unimodal (log-normal) and associated with submicron aerosols of about 0.5 to 0.6  $\mu\text{m}$ . On average, the AMAD of  $^{210}\text{Pb}$ -aerosols (0.53  $\mu\text{m}$ ) has been found to be significantly lower than the average mass median aerodynamic diameter "MMAD" (0.675  $\mu\text{m}$ ), and higher than or at most equal to the respective surface median aerodynamic diameter "SMAD" (0.465  $\mu\text{m}$ ) of the aerosols, i.e. SMAD < AMAD < MMAD. Variation of the atmospheric processes resulted in a variability of the AMAD, between 0.28 and 0.74  $\mu\text{m}$  for  $^{210}\text{Pb}$ -aerosols. While in the winter period (October to April) the AMAD values of  $^{210}\text{Pb}$ -aerosols averaged 0.595  $\mu\text{m}$ , in the summer period  $^{210}\text{Pb}$  was associated with significantly smaller-sized aerosols (AMAD: 0.43  $\mu\text{m}$ ).

Suzuki *et al.* (1999) by using a 40-cfm high-volume cascade impactor with five stages reported that 77% of  $^{210}\text{Pb}$ - and 70% of  $^{210}\text{Po}$ -activities were measured in size-fractionated aerosols with a diameter smaller than 0.70  $\mu\text{m}$  from the west coast of the Japanese Islands ( $38^{\circ}46'\text{N}$ ,  $139^{\circ}44'\text{E}$ ).

Apart of this, Papastefanou (2008) estimated the AMAD of another radionuclide in ambient aerosols, that is  $^7\text{Be}$  ( $T_{1/2} = 53.3$  days) of cosmogenic origin, varying between 0.76 and 1.18  $\mu\text{m}$  (average 0.90  $\mu\text{m}$ ) in the accumulation mode of the activity size distribution of aerosol particles. The aerodynamic size

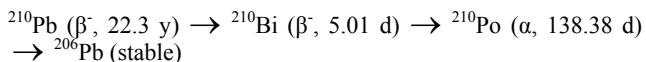
**Table 1.** Activity median aerodynamic diameters (AMADs) of radon decay product aerosols.

$^{214}\text{Pb}$ AMADs ( $\mu\text{m}$ )	$^{212}\text{Pb}$ AMADs ( $\mu\text{m}$ )	$^{210}\text{Pb}$ AMADs ( $\mu\text{m}$ )	Reference
0.10-0.37 (avg. 0.16)	0.07-0.25 (avg. 0.12)	0.28-0.49 (avg. 0.37)	This work
-	0.42	0.56	Grundel and Porstendörfer (2004)
-	-	0.28-0.74 (avg. 0.53)	Winkler <i>et al.</i> (1998)
0.26-0.46 (avg. 0.38)	-	-	El Hussein and Ahmed (1995)
0.18-0.49 (avg. 0.33)	-	-	El Hussein <i>et al.</i> (1998)
0.30-0.36 (avg. 0.32)	0.25-0.39 (avg. 0.36)	-	Mohammed (1999)
-	-	0.70	Suzuki <i>et al.</i> (1999)

distribution of  ${}^7\text{Be}$  in atmospheric aerosols and then the AMAD was achieved by using Andersen 1-ACFM cascade impactors, in association with a gamma-ray spectrometer linked with a Ge coaxial-type detector for the  ${}^7\text{Be}$  activity measurement of the collection plates and the back up filter of the impactor.

### Residence Times of Radon Decay Product Aerosols

The method for estimating the residence time of atmospheric aerosol particles associated with the radon decay product radionuclides is based on the radioactivity of a pair of genetically related radioisotopes, such as  ${}^{210}\text{Pb}$ ,  ${}^{210}\text{Bi}$  and or  ${}^{210}\text{Pb}$ ,  ${}^{210}\text{Po}$ , according to the sequential disintegrations in the  $\beta$ -decay scheme



The residence time,  $\tau_R$  is described by the formula

$$\tau_R = 1/\lambda_{\text{Bi}} \cdot \frac{\lambda_{\text{Bi}} N_{\text{Bi}} / \lambda_{\text{Pb}} N_{\text{Pb}}}{1 - (\lambda_{\text{Bi}} N_{\text{Bi}} / \lambda_{\text{Pb}} N_{\text{Pb}})} \quad (1)$$

where  $\lambda_{\text{Bi}} N_{\text{Bi}}$  is the activity of  ${}^{210}\text{Bi}$ ,  $\lambda_{\text{Pb}} N_{\text{Pb}}$  is the activity of  ${}^{210}\text{Pb}$  in air and  $\lambda_{\text{Bi}} = 0.138 \text{ d}^{-1}$  is the decay constant of  ${}^{210}\text{Bi}$ .

The Eq. (1) was derived from the equation of the production and removal of radionuclides assuming a steady state equilibrium

$$dN_{\text{Bi}}/dt = \lambda_{\text{Pb}} N_{\text{Pb}} - (\lambda_{\text{Bi}} + \lambda_R) \cdot N_{\text{Bi}} = 0 \quad (2)$$

where  $\lambda_R = 1/\tau_R$  is the first-order rate constant for the removal of aerosol particles from the atmosphere by all processes, that is the inverse of residence time,  $\tau_R$ .

The ratio of the activities  $\lambda_{\text{Bi}} N_{\text{Bi}} / \lambda_{\text{Pb}} N_{\text{Pb}}$  in Eq. (1) varied from 0.40 to 0.68 (this work) or from 0.42 to 0.85 (Moore *et al.*, 1972).

If the activity of  ${}^{210}\text{Po}$ ,  $\lambda_{\text{Po}} N_{\text{Po}}$  in air is considered and  $\lambda_{\text{Po}} = 5.0 \times 10^{-3}/\text{d}$  is the decay constant of  ${}^{210}\text{Po}$ , then the activity ratio of  ${}^{210}\text{Po}$ ,  $\lambda_{\text{Po}} N_{\text{Po}}$  and  ${}^{210}\text{Pb}$ ,  $\lambda_{\text{Pb}} N_{\text{Pb}}$  is given by the equation

$$\lambda_{\text{Po}} N_{\text{Po}} / \lambda_{\text{Pb}} N_{\text{Pb}} = \frac{\tau_R^2}{(\tau_R + 1/\lambda_{\text{Bi}}) \cdot (\tau_R + 1/\lambda_{\text{Po}})} \quad (3)$$

from which the residence time,  $\tau_R$  is determined as

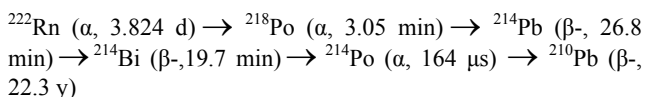
$$\tau_R = \frac{-b + (b^2 - 4ac)^{1/2}}{2a} \quad (4)$$

where

$$\begin{aligned} a &= \lambda_{\text{Pb}} N_{\text{Pb}} - \lambda_{\text{Po}} N_{\text{Po}} \\ b &= c \lambda_{\text{Pb}} N_{\text{Pb}} \cdot (1/\lambda_{\text{Bi}} + 1/\lambda_{\text{Po}}) \\ c &= -\lambda_{\text{Po}} N_{\text{Po}} \cdot (1/\lambda_{\text{Bi}} \lambda_{\text{Po}}) \\ \lambda_{\text{Bi}} &= 0.138/\text{d} \text{ and } \lambda_{\text{Po}} = 5 \times 10^{-3}/\text{d} \end{aligned} \quad (5)$$

The ratio of the activities  $\lambda_{\text{Po}} N_{\text{Po}} / \lambda_{\text{Pb}} N_{\text{Pb}}$  in Eq. (3) varied from 0.054 to 0.092 (Moore *et al.*, 1972).

The residence time,  $\tau_R$  can also be determined through the ratio of the activities of radon,  ${}^{222}\text{Rn}$ ,  $\lambda_{\text{Rn}} N_{\text{Rn}}$  and  ${}^{210}\text{Pb}$ ,  $\lambda_{\text{Pb}} N_{\text{Pb}}$  in air according to the sequential disintegrations in the  $\alpha$ - and  $\beta$ -decay scheme as



and the Eq. (2) by the formula

$$\tau_R = 1/\lambda_{\text{Pb}} \cdot \frac{1}{(\lambda_{\text{Rn}} N_{\text{Rn}} / \lambda_{\text{Pb}} N_{\text{Pb}}) - 1} = 1/\lambda_{\text{Pb}} \cdot (\lambda_{\text{Pb}} N_{\text{Pb}} / \lambda_{\text{Rn}} N_{\text{Rn}}) \quad (6)$$

where  $\lambda_{\text{Pb}} = 8.5 \times 10^{-5}/\text{d}$  is the decay constant of  ${}^{210}\text{Pb}$  and  $\lambda_{\text{Rn}} N_{\text{Rn}} / \lambda_{\text{Pb}} N_{\text{Pb}} \gg 1$ .

The ratio of the activities  $\lambda_{\text{Rn}} N_{\text{Rn}} / \lambda_{\text{Pb}} N_{\text{Pb}}$  in Eq. 6 varied from 282 to 7700 (Moore *et al.*, 1972).

Taking into account the  ${}^{210}\text{Bi}/{}^{210}\text{Pb}$  ratios as determined in twenty one measurements of aerosol samplings carried out during an annual period at Oak Ridge, Tennessee at temperate latitude ( $35^\circ 58' \text{N}$ ,  $84^\circ 17' \text{W}$ ) with high precipitation (wet climate), the estimated residence time of atmospheric aerosols in the boundary layer varied from 4.8 to 15.3 days (average 8.2 days).

Table 2 shows data for the residence times,  $\tau_R$  of atmospheric aerosol particles associated with radon,  ${}^{222}\text{Rn}$  and radon decay products  ${}^{210}\text{Pb}$ ,  ${}^{210}\text{Bi}$  and  ${}^{210}\text{Po}$ . The reported from the literature  $\tau_R$  values are also shown in Table 2 and analyzed as follows:

Poet *et al.* (1972) estimated tropospheric aerosol residence times ranging from 1.59 to 13 days (average 5.4 days) when based on the  ${}^{210}\text{Bi}/{}^{210}\text{Pb}$  activity ratios and from 11 to 77 days (average 24 days) when based on the  ${}^{210}\text{Po}/{}^{210}\text{Pb}$  activity ratios for twenty measurements of aerosol samplings carried out in surface air during a 4 1/2-year period at Boulder, Colorado ( $40^\circ 01' \text{N}$ ,  $105^\circ 17' \text{W}$ ). They concluded that, a mean tropospheric residence time of about 4 days could be applied for aerosol particles in the lower troposphere and about a week for aerosol particles in precipitation. They also found that the mean aerosol residence time increases with altitude within troposphere less than by a factor of 3 (Moore *et al.*, 1973).

Francis *et al.* (1970) estimated a mean atmospheric residence time for  ${}^{210}\text{Pb}$  of 9.6 days  $\pm 20\%$  based on the  ${}^{210}\text{Po}/{}^{210}\text{Pb}$  activity ratios from the dust of filtrate ( $> 0.22 \text{ } \mu\text{m}$ ) collected during a 3-month period (May-August) at Madison, Wisconsin ( $43^\circ 05' \text{N}$ ,  $89^\circ 22' \text{W}$ ).

Marley *et al.* (2000) estimated residence times for seven aerosol samples collected at Argonne, Illinois ( $41.7^\circ \text{N}$ ,  $88.0^\circ \text{W}$ ) during a 2-year period, three aerosol samples collected at Phoenix, Arizona, one sample collected at Socorro, New Mexico, and five samples collected at Mexico city, Mexico. Based on the  ${}^{210}\text{Bi}/{}^{210}\text{Pb}$  activity ratios, they resulted in residence times of 6 to 67 days, while based on the  ${}^{210}\text{Po}/{}^{210}\text{Pb}$  activity ratios, they suggested residence times of 33 to 66 days for the aerosols below  $2 \text{ } \mu\text{m}$  in size.

Much earlier, Fry and Menon (1962) in twelve measurements carried out during a 7-month period (spring and summer) at Fayetteville, Arkansas ( $36^\circ 03' \text{N}$ ,  $78^\circ 54' \text{W}$ ), indicated apparent aerosol residence times ranging from 2.4 to 25.6 days (average 8.5 days), based on the  ${}^{210}\text{Bi}/{}^{210}\text{Pb}$  activity ratios in Arkansas rains. Gavini *et al.* (1974) also estimated residence times varied from 3 to 240 days (average 29 days) from the  ${}^{210}\text{Bi}/{}^{210}\text{Pb}$  activity ratios in Arkansas rains also.

Baskaran and Shaw (2001) based on the  ${}^{210}\text{Po}/{}^{210}\text{Pb}$  activity ratios estimated residence times of arctic haze aerosols, from the upper atmosphere to the arctic atmosphere, varied between 12 and 32 days from the measurements carried out during an 1 1/2 - year period (winter) at Poker Flat ( $65.1^\circ \text{N}$ ,  $147.5^\circ \text{W}$ ) and between 0 and 39 days from eight measurements carried out during a 2-month period (winter) at Eagle ( $69.5^\circ \text{N}$ ,  $141.2^\circ \text{W}$ ) in Alaska.

Very early, Lehman and Sittkus (1959) estimated aerosol residence times of 20 days from the  ${}^{210}\text{Po}/{}^{210}\text{Pb}$  activity ratios in air at Freiburg, Germany ( $47^\circ 59' \text{N}$ ,  $7^\circ 51' \text{E}$ ), while Peirson *et al.* (1966) estimated aerosol residence times of 40 days from the  ${}^{210}\text{Po}/{}^{210}\text{Pb}$  activity ratios in air at Milford Haven, Wales ( $51^\circ 40' \text{N}$ ,  $5^\circ 02' \text{E}$ ). Lambert *et al.* (1980) estimated aerosol

**Table 2.** Residence times,  $\tau_R$  of tropospheric aerosols (days).

Investigation	$^{210}\text{Bi}/^{210}\text{Pb}$	$^{210}\text{Po}/^{210}\text{Pb}$	$^{222}\text{Rn}/^{210}\text{Pb}$	Reference
Oak Ridge, Tennessee (35°58'N, 84°30'W)	4.8-15.3 (avg. 8.2)	-	-	This work
Boulder, Colorado (40°01'N, 105°17'W)	1.59-13.0 (avg. 5.4)	11-37	-	Poet <i>et al.</i> (1972)
Argonne, Illinois (41.7°N, 88.0°W)	-	-	2.2,3.4	Moore <i>et al.</i> (1972)
Madison, Wisconsin (43°05'N, 89°22'W)	6-67	33-66	-	Marley <i>et al.</i> (2000)
Fayetteville, Arkansas (35°03'N, 78°54'W)	-	9.6	-	Francis <i>et al.</i> (1970)
Poker Flat, Alaska (65.1°N, 147.2°W)	2.4-25.6 (avg. 8.5)	-	-	Fry and Menon (1962)
Eagle, Alaska (69.5°N, 141.2°W)	3-240 (avg. 20)	2-320 (avg. 40)	-	Gavini <i>et al.</i> (1974)
Jungfrauoch, Switzerland (46°32'N, 07°59'E)	-	11.9-32	-	Baskaran and Shaw (2001)
Freiburg, Germany (47°59'N, 7°51'E)	-	0-38.9	-	
Gif-sur-Yvette, France (48°52'N, 2°20'E)	-	1-12 (avg. 6)	-	Gäggeler <i>et al.</i> (1995)
Milford Haven, Wales (51°40'N, 5°02'W)	-	20	-	Lehmann and Sittkus (1959)
Bombay, India (18°58'N, 72°50'E)	8.8-10.5	-	6.5	Lambert <i>et al.</i> (1980)
El-Minia, Egypt (28°04'N, 30°45'E)	7-9	40	6.77	Lambert <i>et al.</i> (1983)
	-	8	-	Peirson <i>et al.</i> (1966)
	8	-	-	Rangarajan (1992)
	4.3-12.8 (avg. 9.83)	-	-	Ahmed <i>et al.</i> (2000)

residence times varied from 8.8 to 10.5 days based on the  $^{210}\text{Bi}/^{210}\text{Pb}$  activity ratios in air, while later in another work they estimated aerosol residence times varied from 7 to 9 days (average 8.58 days) based on the  $^{210}\text{Bi}/^{210}\text{Pb}$  activity ratios in air, in near Paris, France area during a 6-year period (Lambert *et al.*, 1983).

Gäggeler *et al.* (1995) during a one-year period carried out measurements on the activities of  $^{214}\text{Pb}$ ,  $^{210}\text{Pb}$  and  $^{212}\text{Pb}$  in air at high altitude in Jungfrauoch, Switzerland (46°32'N, 07°59'E) as high as 3450 m by using an epiphaniometer. They estimated aerosol residence times varied between 1 and 12 days (average 6 days) from the  $^{214}\text{Pb}/^{210}\text{Pb}$  activity ratios.

Finally, Rangarajan (1992) based in the  $^{210}\text{Bi}/^{210}\text{Pb}$  activity ratios in air estimated a mean residence time of the natural radioactive aerosols in the planetary boundary layer at Bombay (Mumbai), India (18°58'N, 72°50'E) around 8 days from forty three measurements carried out during the long dry period, from October to May.

The data of Table 2 admit residence times of lower values as low as 1.59 days and higher values as high as 320 days. Mostly, the lower  $\tau_R$ -values were resulted from the  $^{210}\text{Bi}/^{210}\text{Pb}$  activity ratios and higher  $\tau_R$ -values from the  $^{210}\text{Po}/^{210}\text{Pb}$  activity ratios. Low  $\tau_R$ -values were also resulted from the  $^{222}\text{Rn}/^{210}\text{Pb}$  activity ratios. Poet *et al.* (1972) concluded that longer apparent residence time values were based on the  $^{210}\text{Po}/^{210}\text{Pb}$  activity ratios, than those based on the  $^{210}\text{Bi}/^{210}\text{Pb}$  activity ratios. The difference may be explained by the presence of a mixture of aerosols of various apparent ages, of which older aerosols (those of greater ages) contribute most of  $^{210}\text{Po}$ . On the other hand, the solid products of radon-decay, that is  $^{210}\text{Pb}$ ,  $^{210}\text{Bi}$  and  $^{210}\text{Po}$  might arise from sources other than radioactive decay within the atmosphere. Poet *et al.* (1972) showed that up to 85% of the  $^{210}\text{Po}$  in the atmosphere is of terrestrial origin, and the vertical profile of  $^{210}\text{Po}$  was found to differ appreciably from that expected from the decay of  $^{222}\text{Rn}$ . Lambert *et al.* (1979) indicated that volcanic gases are very rich in long-lived radon decay products, especially

in  $^{210}\text{Po}$  relative to  $^{210}\text{Pb}$ . Soil particles are the most likely contributors, since a part of the tropospheric aerosols originates at the Earth's surface. Coal burning and forests fires presumably are additional sources of radionuclides.

Apart of this, Papastefanou (2008) estimated the residence times of another radionuclide in ambient aerosols, that is  $^7\text{Be}$  ( $T_{1/2} = 53.3$  d) of cosmogenic origin varying between 7.4 and 8.9 days (average 8 days) at Thessaloniki, Greece (40°38'N, 22°58'E) in the category of the lower values of the residence times of atmospheric aerosols and leading to the same result for the residence times of radon decay product aerosols in ambient air varying between 4.8 and 15.3 days (average 8.2 days). The method used for the determination of the residence time of  $^7\text{Be}$  aerosols was described elsewhere (Papastefanou, 2008).

## CONCLUSIONS

The aerodynamic size distributions of radon decay product aerosols in ambient air were measured using low-pressure (LPI) and conventional (1-ACFM) and/or high volume (HVI) cascade impactors. Lead-214 and  $^{212}\text{Pb}$  were largely associated with aerosol particles in the accumulation mode for smaller than 0.52  $\mu\text{m}$  diameter particles in size. Based on the 46 % low-pressure impactor measurements, the mean activity median aerodynamic diameter "AMAD" of  $^{214}\text{Pb}$ -aerosols was found to be 0.16  $\mu\text{m}$ , while for the  $^{212}\text{Pb}$ -aerosols, the mean AMAD was found to be 0.12  $\mu\text{m}$ . The slightly larger size of  $^{214}\text{Pb}$ -aerosol particles confirmed with operationally different cascade impactors, was attributed to  $\alpha$ -recoil-driven redistribution of  $^{214}\text{Pb}$  following the decay of the aerosol-associated  $^{218}\text{Po}$ . Even considering recoil following  $^{214}\text{Po}$   $\alpha$ -decay, the average  $^{210}\text{Pb}$ -labelled aerosols grow by a factor of two during its atmospheric lifetime. Estimated lifetimes of radon decay product aerosols in ambient air resulted in a mean residence time of about 8 days that could be applied to aerosol particles in the lower atmosphere below the boundary layer.

## NOMENCLATURE

1-ACFM	normal flow rate cascade impactor
AMAD	activity median aerodynamic diameter
cfm	cubic feet per meter
$D_p$	particle diameter
ECD	effective cutoff diameter
HVI	high-volume cascade impactor
LPI	low-pressure cascade impactor
M	molar solution
MMAD	mass median aerodynamic diameter
N	number of radioactive nuclei
OLACI	on-line alpha cascade impactor
SMAD	surface median aerodynamic diameter

## Greek symbols

$\lambda$	radioisotope disintegration rate
$\sigma_g$	geometric standard deviation
$\tau$	radioisotope mean life
$\tau_R$	residence time of aerosol particles

## REFERENCES

- Ahmed, A.A., Mohammed, A., Ali, A.A., El-Hussein, A. and Barakat, A. (2000). A study on Aerosol Residence Time in El-Minia, Egypt. *J. Aerosol Sci.* 31: 470-471.
- Baskaran, M. and Shaw, G.E. (2001). Residence Time of Arctic Haze Aerosols Using the Concentrations and Activity Ratios of  $^{210}\text{Po}$ ,  $^{210}\text{Pb}$  and  $^7\text{Be}$ . *J. Aerosol Sci.* 32: 443-452.
- El-Hussein, A. and Ahmed, A.A. (1995). Unattached Fraction and Size Distribution of Aerosol-attached Radon Progeny in the Open Air. *Appl. Radiat. Isot.* 46: 1393-1399.
- El-Hussein, A., Mohammed, A. and Ahmed, A.A. (1998). A Study on Radon and Radon Progeny in Surface Air of El-Minia, Egypt. *Radiat. Prot. Dosim.* 78: 139-145.
- Francis, C.W., Chesters, G. and Haskin, L.A. (1970). Determination of  $^{210}\text{Pb}$  Mean Residence Time in the Atmosphere. *Environ. Sci. Technol.* 4: 586-589.
- Friedlander, S.G. (2000). *Smoke, Dust, and Haze: Fundamentals of Aerosol Dynamics*. 2<sup>nd</sup> Edn. Oxford University Press, New York.
- Fry, L.M. and Menon, K.K. (1962). Determination of the Tropospheric Residence Time of Lead-210. *Science*. 137: 994-995.
- Gäggeler, H.W., Jost, D.T., Baltensperger, U. and Schwikowski, M. (1995). Radon and Thoron Decay Product and  $^{210}\text{Pb}$  Measurements at Jungfraujoch, Switzerland. *Atmos. Environ.* 29: 607-616.
- Gavini, M.B., Beck, J.N. and Kuroda, P.K. (1974). Mean Residence Times of the Long-lived Radon Daughters in the Atmosphere. *J. Geophys. Res.* 79: 4447-4452.
- George, A.C. and Breslin, A.J. (1980). The Distribution of Ambient Radon and Radon Daughters in Residential Buildings in the New Jersey-New York Area. *Proceedings of the 3<sup>rd</sup> International Symposium on Natural Radiation Environment*, CONF-780422, Vol. 2, p. 1272-1292, National Technical Information Service, Springfield, Va.
- George, A.C., Knutson, E.O., Sinclair, D., Wilkening, M.H. and Andrews, L. (1984). Measurements of Radon Daughter Aerosols in Socorro, New Mexico. *Aerosol Sci. Technol.* 3: 277-281.
- Grundel, M. and Porstendörfer, J. (2004). Differences between the Activity Size Distributions of the Different Natural Radionuclide Aerosols in Outdoor Air. *Atmos. Environ.* 38: 3723-3728.
- Jaworowski, Z. (1963). *Air Chemistry and Radioactivity*. Academic Press, New York.
- Lambert, G., Buisson, A., Sanak, J. and Ardouin, B. (1979). Modification of the Atmospheric Polonium-210 to Lead-210 Ratio by Volcanic Emissions. *J. Geophys. Res.* 84: 6980-6986.
- Lambert, G., Ardouin, B., Buisson, A., Jegou, A., Le Roulley, J.C., Polian, G. and Sanak, J. (1980). *Cycle De Radon Et De Aes Descendants: Applications a L'etude Des Echanges Troposphere-stratosphere*. C.R Fin d'etude De Recherché DGRST.
- Lambert, G., Sanak, J. and Polian, G. (1983). Mean Residence Time of Submicrometer Aerosols in the Global Troposphere. *Precipitation Scavenging, Dry Deposition and Resuspension*. Pruppacher, H.R., Semonin, R.G. and Slinn, W.G.N. (Ed.), Elsevier, New York, p. 1353-1359.
- Lehmann, L. and Sittkus, A. (1959). Bestimmung Von Aerosolverweilzeiten Aus Fen RaD Und RaF-Gehalt Der Atmosphärischen Luft Und Des Niederschlages. *Naturwissenschaft.* 46: 9-10.
- Marley, N.A., Gaffney, J.S., Drayton, P.J., Cunningham, M.M., Orlandini, K.A. and Paode, R. (2000). Measurement of  $^{210}\text{Pb}$ ,  $^{210}\text{Po}$  and  $^{210}\text{Bi}$  in Size-fractionated Atmospheric Aerosols: An Estimate of Fine-aerosol Residence Times. *Aerosol Sci. Technol.* 32: 569-583.
- Mercer, T. (1976). The Effect of Particle Size on the Escape of Recoiling RaB Atoms from Particulate Surfaces. *Health Phys.* 31: 173-175.
- Mohammed, A. (1999). Activity Size Distributions of Short-lived Radon Progeny in Indoor Air. *Radiat. Prot. Dosim.* 86: 139-145.
- Mohammed, A., El-Hussein, A. and Ali, A.E. (2000). Measurements of Thorium-B ( $^{212}\text{Pb}$ ) in the Outdoor Environment and Evaluation of Equivalent Dose. *J. Environ. Radioact.* 49: 181-193.
- Moore, H.E., Poet, S.E. and Martell, E.A. (1972). Tropospheric Aerosol Residence Times Indicated by Radon and Radon-Daughter Concentrations. *Natural Radiation Environment II*. Adams J.A.S., Lowder, W.M. and Gessel, T.F. (Ed.). CONF-720805-P2, Technical Information Center/U.S. Department of Energy, Washington, D.D. p. 775-786.
- Moore, H.E., Poet, S.E. and Martell, E.A. (1973).  $^{222}\text{Rn}$ ,  $^{210}\text{Pb}$ ,  $^{210}\text{Bi}$  and  $^{210}\text{Po}$  Profiles and Aerosol Residence Times Versus Altitudes. *J. Geophys. Res.* 78: 7065-7075.
- Papastefanou, C. (2008). Beryllium-7 Aerosols in Ambient Air. *Aerosol Air Qual. Res.* 9: 187-197.
- Peirson, D.H., Cambrey, R.S. and Spicer, G.S. (1966). Lead-210 and Polonium-210 in the Atmosphere. *Tellus*. 18: 427-433.
- Poet, S.E., Moore, H.E. and Martell, E.A. (1972). Lead-210,  $^{210}\text{Bi}$ , and  $^{210}\text{Po}$  in the Atmosphere: Accurate Ratio and Application to Aerosol Residence Time Determination. *J. Geophys. Res.* 77: 6515-6527.
- Porstendörfer, J. and Mercer, T. (1980). Diffusion Coefficient of Radon Decay Products and their Attachment Rate to the Atmospheric Aerosol. *Natural Radiation Environment III*. Gesell, T.F. and Lowder, W.M. (Ed.) CONF.780422, Vol. 1, National Technical Information Service, Springfield, Virginia, p. 281-293.
- Rangarajan, C. (1992). A Study of the Mean Residence Time of the Natural Radioactive Aerosols in the Planetary Boundary Layer. *J. Environ. Radioact.* 15: 193-206.
- Röbig, G., Becker, K.H., Hessin, A. and Porstendörfer, J. (1980). A Cascade Impactor Calibration for Measurement of Activity Size Distributions in the Atmosphere. *Proceedings of the 8<sup>th</sup> Conference in Aerosol Science*, Georg-August-University, Göttingen, Germany, p. 96-102.
- Soilleux, P.J. (1970). The Measurement of the Size Spectrum and Charge to Total Ratio of Condensation Nuclei Having Naturally Occurring Radon Daughter Products Attached to Them. *Health Phys.* 12: 245-254.

Suzuki, T., Maruyama, Y., Nakayama, N., Yamada, K. and Ohta, K. (1999). Measurement the  $^{210}\text{Po}/^{210}\text{Pb}$  Activity Ratio in Size Fractionated Aerosols from the Coast of Japan Sea. *Atmos. Environ.* 33: 2285-2288.

Winkler, R., Dietl, F., Frank, G. and Tschiersch, J. (1998).

Temporal Variation of  $^7\text{Be}$  and  $^{210}\text{Pb}$  Size Distributions in Smbient Aerosol. *Atmos. Environ.* 32: 983-991.

*Received for review, February 6, 2009*

*Accepted, April 10, 2009*